On the Comparative Performance Analysis of Turbo-Coded Non-Ideal Single-Carrier and Multi-Carrier Waveforms over Wideband Vogler-Hoffmeyer HF Channels

Fatih GENÇ[1], M. Anıl REŞAT[2], Asuman SAVAŞÇIHABEŞ[3], Özgür ERTUĞ[4]

[1] CU OPEN Lab, Dept. of Electronic and Communication Engineering, Çankaya University,Yukarıyurtçu Mahallesi Mimar Sinan Caddesi No:4, 06790, Etimesgut, Ankara, Turkey

[2] Dept. of Electrical and Electronics Engineering, Yıldırım Beyazıt University, Çankırı Caddesi Çiçek sok. No:3 , Altındağ, Ankara, Turkey

[3] Dept. of Electrical and Electronics Engineering, Nuh Naci Yazgan University, Erkilet Dere Mah., Kocasinan, Kayseri/Turkey

[4] Telecommunication and Signal Processing Laboratory, Dept. of Electrical and Electronics Engineering, Gazi University, Yükseliş Sk. No:5, Maltepe, Ankara/Turkey

c1182604@student.cankaya.edu.tr, anilresat@yahoo.com, asavascihabes@gazi.edu.tr, ertug@gazi.edu.tr

Abstract. *The purpose of this paper is to compare the turbo-coded Orthogonal Frequency Division Multiplexing (OFDM) and turbo-coded Single Carrier Frequency Domain Equalization (SC-FDE) systems under the effects of Carrier Frequency Offset (CFO), Symbol Timing Offset (STO) and phase noise in wide-band Vogler-Hoffmeyer HF channel model. In mobile communication systems multipath propagation occurs. Therefore channel estimation and equalization is additionally necessary. Furthermore a non-ideal local oscillator generally is misaligned with the operating frequency at the receiver. This causes carrier frequency offset. Hence in coded SC-FDE and coded OFDM systems; a very efficient, low complex frequency domain channel estimation and equalization is implemented in this paper. Also Cyclic Prefix (CP) based synchronization synchronizes the clock and carrier frequency offset. The simulations show that non-ideal turbo-coded OFDM has better performance with greater diversity than non-ideal turbo-coded SC-FDE system in HF channel.*

Keywords

SC-FDE, OFDM, FFT-based channel estimation, ML synchronization, HF channel.

1. Introduction

Spectral and power efficiency of terminal in the limited bandwidth and transmit power have been developing continuously for the new generation of wireless communication systems. To meet the new user demands new air interfaces are needed to be enhanced. Orthogonal Frequency-Division Multiplexing (OFDM) is a popular modulation technique to satisfy these requirements, adopted to broadcast systems, such as Digital Video Broadcasting (DVB) [13], Digital Audio Broadcasting (DAB), Wireless Local Area Networks (WLAN) and Asymmetric Digital Subscriber Line (ADSL) for wired systems. In OFDM systems, one Inverse Fast-Fourier Transform (IFFT) block is used at the transmitter and also one FFT block is used at the receiver sides of the link. In the IFFT block, OFDM transmitter multiplexes the information into many low-rate streams which are transmitted parallelly instead of sending the information as a single stream [1],[16]. The modulated signals in an OFDM system have high peak values in time domain since many sub-carriers are added via an IFFT operation. Therefore, OFDM systems are known to have high Peak-to-Average Power Ratio (PAPR). Due to the limited battery life in mobile terminals, the PAPR problem is a main disadvantage of the OFDM system for the up-link [14].

On the other hand, Single-Carrier Frequency-Domain Equalization (SC-FDE) is a desirable alternative to OFDM systems. In the case of SC-FDE technique, no IFFT and FFT blocks exist at the transmit side while FFT and IFFT operators are performed at the receiver side of the link. SC-FDE experiences lower PAPR levels than OFDM because no IFFT is performed at the transmitter to precode the signal. In order to mitigate the PAPR problem, Single-Carrier (SC) transmission uses single-carrier modulation instead of many sub-carriers [1]-[3].

Low-complexity channel equalization and estimation in the frequency domain are used to mitigate the inter-symbol interference (ISI) [4]. For this purpose, frequency

domain MMSE equalizer is generally used to minimize the attenuations of the fading channel. For wide-band channels, conventional time domain equalizers are impractical because of the very long channel impulse response in the time domain. Frequency domain equalization is more practical for such channels because the FFT size does not grow linearly with the length of the channel response and the complexity of the FDE is much lower than the time domain equalizer.

At the same time, frequency domain MMSE estimation is preferred with the comb-type pilot tone arrangement to predict the multi-path channel coefficients [9]-[11]. In order to estimate the channel characteristics, the comb-type pilot symbols are placed as periodically as possible in coherence time. The coherence time is the inverse of the Doppler spread in the channel.

An additional way to eliminate ISI almost completely, is to use a guard interval which is called cyclic-prefix (CP). The CP is the replica of the last L symbols of the block as shown in Fig. 4. The guard time L must be larger than the expected channel delay spread. At the receiver, the received CP is discarded before processing the block. By doing so CP also prevents inter-block interference.

CP is also used in CP-based channel synchronization to compensate the inter-carrier interference (ICI) caused by the Doppler effect [15],[16]. CP-based synchronization enables CFO estimation without need of additional redundant pilots. In fact, the key point is that CP already contains sufficient information to perform synchronization. Without CFO, the sub-channels do not interfere with one another. The impact of frequency offset is loss of orthogonality between the tones. Hence, the received signal is not a white process because of its probabilistic structure and it contains information about the timing offset and carrier frequency offset [12]. Estimations of timing offset θ and frequency offset $\hat{\varepsilon}$ are achieved by the relation of the CPs of consecutive frames.

In this paper, the performances of the turbo-coded SC-FDE and OFDM systems in wide-band Vogler-Hoffmeyer HF channels are compared. In practice, a wide-band radio channel has time-variant, frequency-selective and noisy properties. Most commonly used HF channel model is recommended by CCIR and ITU-R that is called as Watterson HF channel [5],[6]. The main restriction of the Watterson model is that the model is designed and tested for narrow-band channels but not for ones having more than 12 kHz bandwidth. In the design of high data speed wide-band HF communication systems, exact modeling and simulation of HF channel are needed. Therefore, Vogler-Hoffmeyer HF channel model is used in this paper [7],[8].

The remainder of this paper is organized as follows. Section II gives an overview of the wide-band Vogler-Hoffmeyer HF channel model. Section III overviews OFDM and SC-FDE structures. In Section IV, channel equalization/estimation and synchronization methods are defined in detail. Numerical results and discussions are given in Sec-

tion V and, finally, conclusions are drawn from the results in Section VI.

2. Wide-Band HF Channel Model

HF channel characteristics are directly shaped by the ionosphere behavior because HF channels utilize the ionospheric reflections in order to provide long-distance communications.

The wide-band HF channel can be modeled as a FIR filter where the taps are time-variant and have complex values. This model can be described by the following equation:

$$y_t = \sum_{i=0}^{L-1} h_i x_t + n_i \qquad (1)$$

where y_t is the complex output of the channel, L is the length of the channel, h_i is one of the L taps of the time-varying transversal filter, x_t is the complex input to the channel and n_i is Additive White Gaussian Noise (AWGN).

This type of a complex-valued FIR filter can be formed easily by convolving the input signal with the channel impulse response. Thus, the coefficients of the filter can be defined as the samples of the HF channel impulse response which is given as:

$$h(t,\tau) = \sqrt{P(\tau)} D(t,\tau) \psi(t,\tau) \qquad (2)$$

where $P(\tau)$ is the delay power profile and its square root $\sqrt{P(\tau)}$ describes the shape in delay dimension; $D(t,\tau)$ is the deterministic phase function showing each path's Doppler shift, and $\psi(t,\tau)$ is the stochastic modulation function which describes the fading value of the impulse response.

The Doppler Effect can also be given with the formula:

$$D(t,\tau) = e^{j2\pi f_D t} \qquad (3)$$

where f_D is the Doppler shift value. The stochastic modulation function $\psi(t,\tau)$ can be stated as random variables with an auto-correlation function that possesses a Gaussian shape.
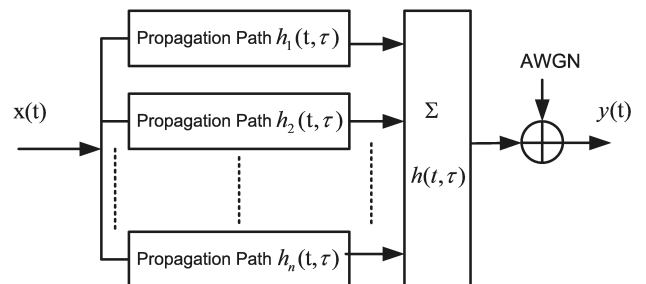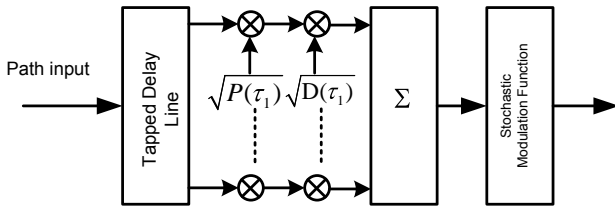

Fig. 1. HF channel model.

Fig. 2. Single propagation path.

Whilst Fig. 1 shows the structure of the wide-band HF channel model with propagation paths, Fig. 2 shows the model of a single propagation path [8]. It is important to specify the main difference between the narrow-band Watterson model and the wide-band channel model here. In the Watterson model time delay spread is neglected and the time delay of each path has a single value. On the other hand, the wide-band model has a delay power profile symbolized with $P(\tau)$ and relates Doppler effect with the time delay of each path.

3. System Models

3.1 OFDM System

In this section OFDM system model is described. The system structure is illustrated in Fig. 3. First, each binary source data are encoded by non-punctured, $R = 1/3$ code-rate turbo encoder and Log-Map algorithm is chosen for best decoding performance with low-complexity for turbo decoder. In this time, N sub-carriers X_k for $k = 0, 1, \ldots, N-1$ are modulated by a signal alphabet $A = \{\pm 1, \pm 3, \pm j, \pm 3j\}$ used for transmitting the information for 16-QAM. After base-band modulation, pilot tone symbol insertion is applied for the channel estimation where the pilot pattern is shown in Fig. 4.
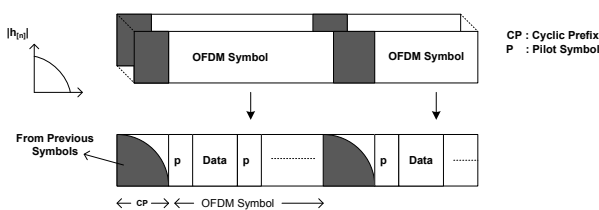

Fig. 4. Frame structure.

Pilot arrangement in OFDM system issue is discussed in more detail under Section IV. Here, output of the IFFT after the serial to parallel conversion can be expressed as:

$$x(n) = \frac{1}{\sqrt{N}} \sum_{k=0}^{N-1} X(k) e^{j2\pi kn/N} \tag{4}$$

where the constant $\frac{1}{\sqrt{N}}$ normalizes the power, N is the sub-carrier number and $X(k)$ are the modulated input symbols.

Cyclic prefix (CP) of length N_c is added at the beginning of the frame which must be greater than the maximum channel delay spread then the composite symbols are transmitted through the HF channel. In order to eliminate inter-carrier interference (ICI), this guard time includes the cyclic

extended part of the OFDM symbol. Next, Root-Raised-Cosine (RRC) pulse shaping filtering is used to reconstruct on the data symbols.

After FFT is applied at the receiver, the received signal is given by:

$$
\begin{aligned}
Y[k] &= \sum_{n=0}^{N-1} y[n] e^{-2\pi kn/N} \\
&= \sum_{n=0}^{N-1} \left\{ \sum_{m=0}^{\infty} h[n] x[n-m] + z[n] \right\} e^{-j2\pi kn/N} \\
&= \sum_{n=0}^{N-1} \left\{ \sum_{m=0}^{\infty} h[m] \left\{ \frac{1}{N} \sum_{i=0}^{N-1} X[i] e^{j2\pi i(n-m)/N} \right\} \right\} e^{-j2\pi kn/N} + Z[k] \\
&= \frac{1}{N} \sum_{i=0}^{N-1} \left\{ \left\{ \sum_{m=0}^{\infty} h[m] e^{-j2\pi im/N} \right\} X[i] \sum_{n=0}^{\infty} e^{-j2\pi(k-i)n/N} \right\} e^{-j2\pi kn/N} \\
&\quad + Z[k],
\end{aligned}
$$

$$Y[k] = H[k]X[k] + Z[k] \tag{5}$$

where $X[k]$ denotes the kth sub-carrier frequency components transmitted symbol, $Y(k)$ is received symbol, $H[k]$ is channel frequency response and $Z[k]$ is noise in frequency domain, respectively.

At the receiver, after passing to discrete-time domain through A/D converter and pulse shaping filter, CP-based ML synchronization is applied to compensate the Carrier Frequency Offset (CFO) which is mentioned in Section IV, then guard time is removed:

$$y[n] = \{y_g(n) \quad M < n < N\} \tag{6}$$

where N is the sub-carrier, M is CP length, y_g received signal that have guard interval insertion.

Then y_n is received to FFT block for the following operation:

$$
\begin{aligned}
Y[k] &= FFT\{y(n)\}, \ k,n = 0,1,\ldots N-1 \\
&= \frac{1}{N} \sum_{n=0}^{N-1} y(n) e^{-j2\pi kn/N}.
\end{aligned} \tag{7}
$$

Next *Least Square* estimated $\hat{H}_{LS}^p[k] = \frac{Y^p[k]}{X^p[k]}$ is obtained by extracting the pilot signals $Y^p[k]$. The interpolated $\hat{H}[k]$ for all data sub-carriers is obtained in MMSE channel estimation. Then, in the Frequency domain equalization (FDE) block the transmitted data is equalized by MMSE equalizer as

$$\hat{X}_n = IFFT\{Y_k C_k\} = y_n \otimes c_n \tag{8}$$

where C_k represents the equalizer correction term, which is computed according to the FDE as follows:

- MMSE Equalizer:

$$C_k = \frac{\hat{H}_{FFT}^*}{\left|\hat{H}_{FFT}\right|^2 + (E_b/N_o)^{-1}} \tag{9}$$

where $(.)^*$ denotes conjugate. MMSE equalizer in (9) makes an optimum trade-off between noise enhancement and channel correction term, while using the signal-to-noise ratio (SNR) value [4]. Finally, the binary information data is obtained back in 16-QAM modulation and turbo decoding respectively.
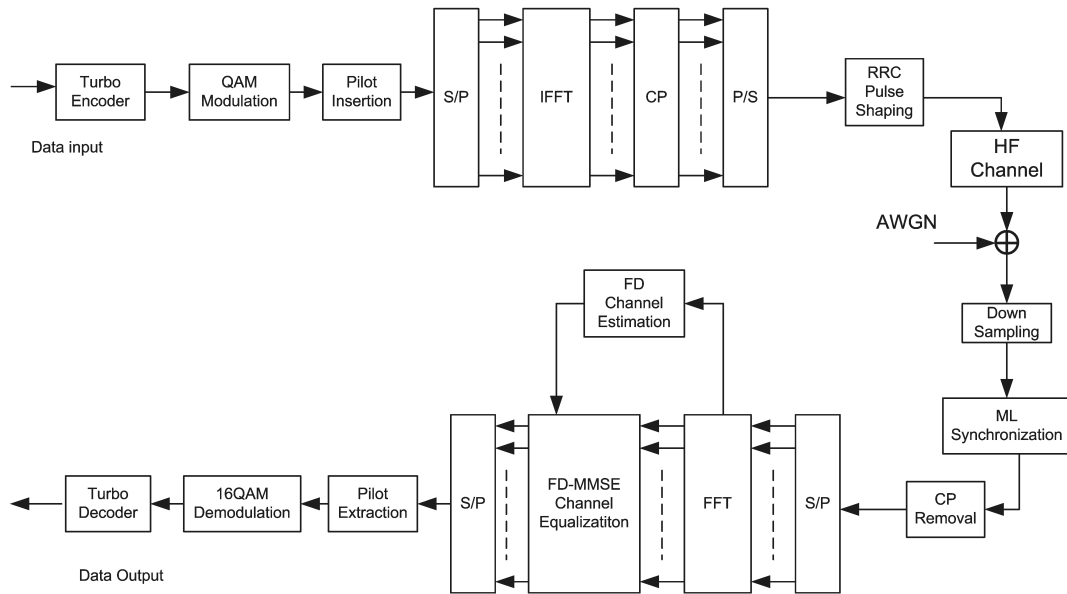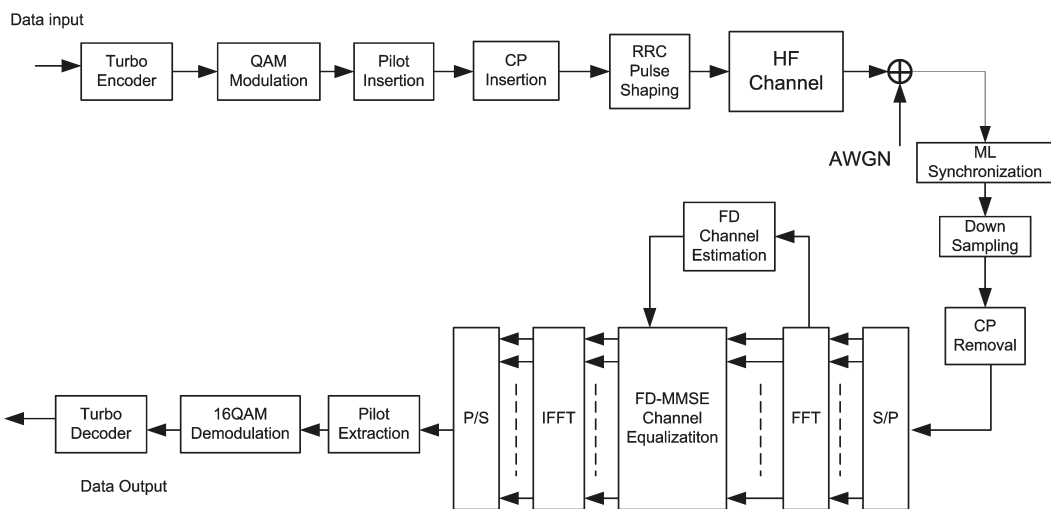
Fig. 3. OFDM structure.

Fig. 5. SC-FDE structure.

3.2 SC-FDE System

OFDM and SC-FDE are similar in many ways. However there are explicit differences that make the two systems perform differently. As shown in Fig. 5, the main difference between OFDM and SC systems is the placement of the IFFT block. In SC systems, it is placed at the receiver side to transform the frequency domain equalized signals, thus compensating for channel distortion, bringing back to the time domain [3]. All the other blocks are formed with the same manner like OFDM system at both sides of the transmission.

In the OFDM system, symbols are exposed to an additional transformation by using the IFFT, $x(n) = IFFT\{X[k]\}$, but in the SC-FDE system no transformation is used. The frame of SC-FDE is transmitted during the time instant after the Turbo encoder, 16-QAM modulation, pilot insertion and CP insertion are applied respectively and the receiver maps received data into the frequency domain in order to equalize. When the channel delay spread is large it is more efficient computationally to equalize in the frequency domain. In addition, SC-FDE has better behavior when used with non-linear power amplifiers.

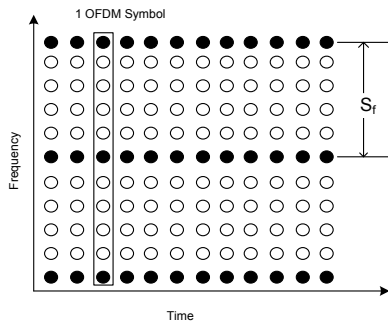# 4. Channel Estimation & Synchronization

4.1 Channel Estimation

Fig. 6. Comb-type pilot arrangement.

Comb-type pilot arrangement, shown in Fig. 6, is used for frequency domain interpolation to estimate channel frequency response that is the Fourier transform of the channel impulse response [9],[10]. In Comb-type pilot arrangement, every OFDM and SC symbol has pilot tones which are periodically located at the sub-carriers. Notice that S_f the periods of pilot tones in frequency domain must be placed in the coherence bandwidth. The coherence bandwidth is determined by an inverse of the *maximum delay spread* σ_{max}. The pilot symbol period is shown as following inequality:

$$S_f = \frac{1}{\sigma_{max}}. \qquad (10)$$

Let us consider the $\hat{H}_{LS} = X^{-1}Y \overset{\triangle}{=} \tilde{H}$, using the weight matrix W channel estimate $\hat{H} \overset{\triangle}{=} W\tilde{H}$ is defined and MSE of the channel estimate is calculated as below :

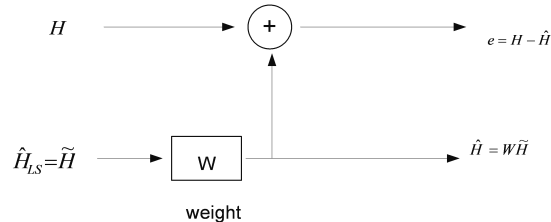$$J(\hat{H}) = E\left\{\|e\|^2\right\} = E\left\{\|H - \hat{H}\|^2\right\}. \qquad (11)$$

Fig. 7. MMSE channel estimation.

MMSE estimation method shown in Fig. 7 finds a better estimate that minimizes the MSE in (11). For the derivation of MMSE channel estimation, the cross-correlation $R_{e\tilde{H}}$, error vector e with channel estimate $\tilde{H}$ is forced to zero.

$$
\begin{aligned}
R_{e\tilde{H}} &= E\left\{e\tilde{H}^H\right\} \\
&= E\left\{(H - \hat{H})\tilde{H}^H\right\} \\
&= E\left\{(H - W\tilde{H})\tilde{H}^H\right\} \\
&= E\left\{H\tilde{H}^H\right\} - WE\left\{\tilde{H}\tilde{H}^H\right\} \\
&= R_{H\tilde{H}} - WR_{\tilde{H}\tilde{H}} = 0
\end{aligned} \qquad (12)
$$

where $(.)^H$ is the *Hermitian* operator. Solving (12) for W yields

$$W = R_{H\tilde{H}}R_{\tilde{H}\tilde{H}}^{-1}. \qquad (13)$$

Using (13) the MMSE channel estimate follows as:

$$\hat{H} = W\tilde{H} = R_{H\tilde{H}}R_{\tilde{H}\tilde{H}}\tilde{H}. \qquad (14)$$
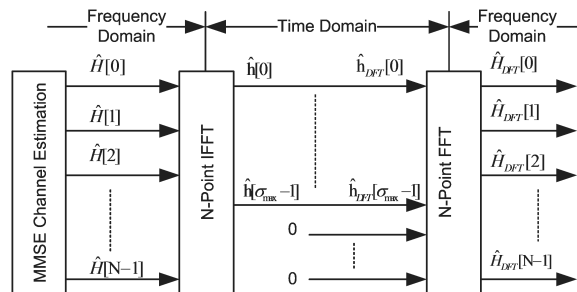

Fig. 8. FFT-based channel estimation.

Fig. 8 shows the block diagram of FFT-based channel estimation, given the MMSE channel estimation. An important point is that σ_{max} must be known formerly to remove the effect of noise outside the channel delay. Taking the IFFT of the MMSE channel estimate $\hat{H}$ to get in the time domain, that the coefficients contain the noise are ignored with zero padding and then transform the remaining σ_{max} elements back to the frequency domain to achieve $\hat{H}_{FFT}$. Finally $\hat{H}_{FFT}$ is used in (9) at the Frequency Domain MMSE Channel Equalizer block.

4.2 Channel Synchronization

In general, there are two types of distortion related to the carrier signal. One is the Phase Noise due to the Voltage Control Oscillator (VCO) and the other is Carrier Frequency

Offset (CFO) caused by Doppler Frequency shift f_d. Let us define the normalized CFO, ε, as a ratio of the CFO to subcarrier spacing Δ_f, i.e.,

$$\varepsilon = \frac{f_d}{\Delta_f} \qquad (15)$$

where f_d is the Doppler Frequency. Here Δ_f is the ratio of the bandwidth to subcarrier number $\left(BW / N_{\Delta f} \right) = \frac{24000}{256} = 93.75$ Hz.

CP-based channel synchronization estimates the time and carrier-frequency offset. This algorithm exploits the cyclic prefix preceding the OFDM and SC symbols, thus reducing the need for pilots. The received data in the time domain are represented by $e^{j2\pi \varepsilon k/N}$, where ε denotes the difference in the transmitter and receiver oscillators as a fraction of the inter-carrier spacing, that is calculated in (15). Notice that all sub-carriers are affected by the same shift ε, shown as:

$$r(k) = s(k-\theta)e^{j2\pi \varepsilon k/N} + n(k) \qquad (16)$$

where $r(k)$ is the received data, $s(k-\theta)$ is the unknown arrival time transmitted signal and $n(k)$ is the AWGN. Hence $r(k)$ contains information about the time offset θ and carrier offset ε. From the observation shown in Fig. 9 the estimation of frequency offset and the estimation of timing offset are calculated as:

$$\gamma(m) \overset{\Delta}{=} \sum_{k=m}^{m+L-1} r(k)r^*(k+N),$$
$$\Phi(m) \overset{\Delta}{=} \frac{1}{2} \sum_{k=m}^{m+L-1} |r(k)|^2 + |r(k+N)|^2, \qquad (17)$$
$$\hat{\theta}_{ML} = \arg\max_{\theta} \left\{ |\gamma(\theta)| - \frac{SNR}{SNR+1}\Phi(\theta) \right\},$$
$$\hat{\varepsilon}_{ML} = -\frac{1}{2}\angle\gamma\left(\hat{\theta}_{ML}\right)$$

where L is the CP length, m is the index of samples, $\gamma(m)$ is the correlation coefficient and $\Phi(m)$ is an energy term [11], [12]. Fig. 9 shows the estimation of timing offsets and frequency offsets. Notice that peaks of the timing estimate, six frame are obtained from the observation interval and the index values of the peaks of the timing estimate gives the estimates of carrier frequency offsets $\hat{\varepsilon}$ values:

$$\hat{\varepsilon} = \hat{\gamma}(maxindexvalues(\hat{\Phi}(m))). \qquad (18)$$
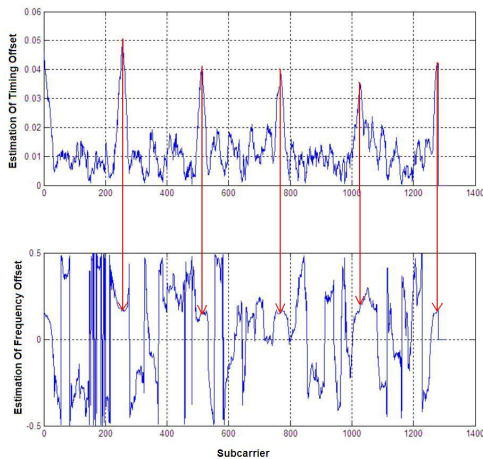

Fig. 9. STO and CFO estimates.

Finally, these estimates are used in channel synchronization block to compensate the carrier frequency offset as:

$$\hat{s}(k) = r(k) \cdot e^{-j2\pi \hat{\varepsilon} k/N} \qquad (19)$$

where $\hat{s}(k)$ is the synchronized signal.

5. Simulation Results

In this section, BER performance of the proposed systems for CFO, STO and phase noise are shown. The simulation parameters are compliant to the wide-band HF channel model: 24 kHz bandwidth, 16 QAM constellation, 256 subcarriers, 210 occupied sub-carriers, 16 cyclic prefix length and pilot tone number is equal to 30. The code rate of the turbo code is $1/3$, the interleaver is 512 block interleaver and 10-iteration log-MAP decoding is used.

In all of the simulations, normalized frequency offset of each system is a constant value between 0.1 and 0.5. For the channel model, multipath Rayleigh fading channel is used which can be modeled as a tapped-delay line with $L_{ch} = 3$ delay taps of [3 7 10] ms. Furthermore the channel gains of the taps are [0 -3 -8] dB .
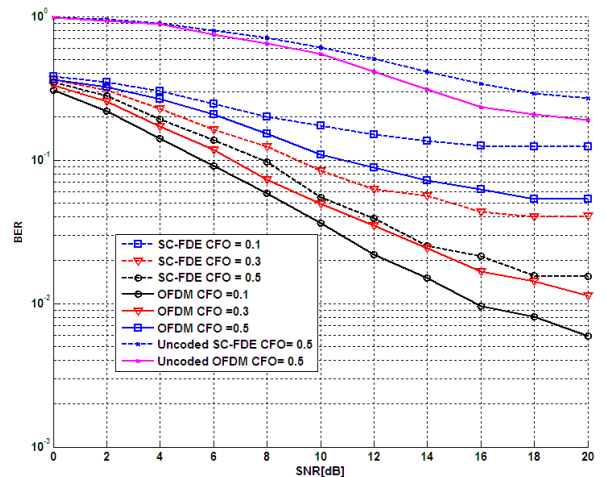

Fig. 10. BER performance versus SNR parametrized by CFO

In the first simulation, the effect of CFO is analyzed. Hence, normalized CFO, ε, is calculated from (15). In this simulation, channel delay spread and phase noise are neglected. As can be seen from Fig. 10, as the frequency offset of the channel increases, BER performances decrease as well. This is because of the way how CFO increments the ICI without the CP-based channel synchronization. Both OFDM and SC-FDE systems experience the impact of severe frequency-selective fading channels even so there are certain contrasts between the performance of their decoders. For lower code rates such as $R = 1/3$ Turbo code, OFDM outperforms SC-FDE. For SC-FDE, the noise amendment loss increases with the average input SNR. When the channel is ineffective and the SNR is high, the equalizer tries to

invert the nulls and, as a result, the noise in these ineffective locations is amplified. Conversely, OFDM combines the useful energy across all sub-carriers through turbo-coding and interleaving.
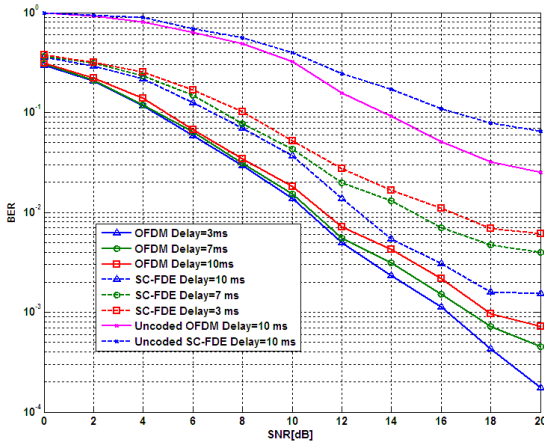

Fig. 11. BER performance versus SNR parametrized by STO.

In the second simulation, the effect of the channel delay spread, that is modeled with zero padding in each propagation path is analyzed. It is assumed that no CFO and phase noise exist. The simulation results are shown in the range of 3 ms to 10 ms channel delay spread. The $R = 1/3$ rate, 4 state (7,5) convolutional turbo encoder has d_{free}. Therefore, a coded OFDM system with this turbo code can achieve a diversity order of 5 without implementing any additional transmit/receive antennas, or using any other diversity techniques. Hence, especially when the channel order is larger, lower rate codes are required to achieve full diversity in OFDM systems. When this is the case, OFDM gives better performance than SC-FDE system because of the reduced effect of ISI.

For the third simulation, the effect of random fluctuations in the phase of a waveform due to the VCO at the -140 dBc/Hz, -100 dBc/Hz, and -70 dBc/Hz values is analyzed. For all simulations it can be seen that increasing the CFO, STO and phase noise effect clearly decreases the system performances especially for SC-FDE.
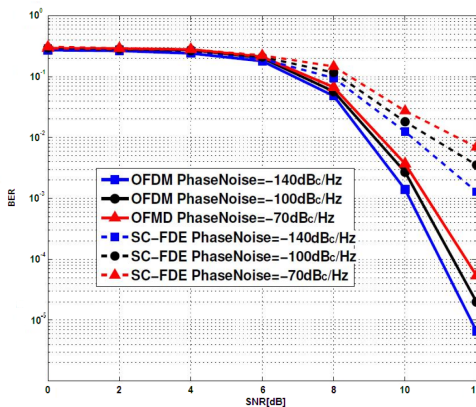

Fig. 12. BER performance versus SNR parametrized by phase noise.

6. Conclusion

In this paper, the performances of the turbo-coded SC and OFDM systems using FDE, MMSE channel estimation, CP-based synchronization over the Wideband Vogler-Hoffmeyer HF channel are simulated. The performance of the proposed systems were compared under only CFO, STO and phase noise effects. The simulation results confirm that turbo-coded OFDM performs significantly better than turbo-coded SC-FDE in HF channel model with the large diversity.

Acknowledgements

References

[1] WEINSTEIN, S. B., et al. Data transmission by frequency-division multiplexing using the discrete Fourier transform. *IEEE Transactions on Communication Technology*, 1971, vol. 19, no. 5, p. 628 - 634.

[2] FALCONER, D., ARIYAVISTAKUL, S. L., BENYAMIN-SEEYAR, A., EDISON, B. Frequency domain equalization for single carrier broadband wireless systems. *IEEE Communications Magazine*, 2002, vol. 40, no. 4, p. 58 - 66.

[3] PANCALDI, F., et al. Single-carrier frequency domain equalization. *IEEE Signal Processing Magazine*, 2008, vol. 25, no. 5, p. 37 - 55.

[4] HASSA, E. S., ZHU, XU, EL-KHAMU, S. E., et al. Enhanced performance of OFDM and single-carrier systems using frequency domain equalization and phase modulation. In *National Radio Science Conference*. New Cairo (Egypt), 2009, p. 1-10.

[5] WATTERSON, C. C., JUROSHEK, J. R., BENSEMA, W. D. Experimental confirmation of an HF channel model. *IEEE Transactions on Communication Techniques*, 1970, vol. 18, no. 6, p. 792 - 803.

[6] HF Ionospheric Channel Simulators, CCIR Report 549-2. *Recommendations and Reports of the CCIR*, vol. 3, p. 59 - 67.

[7] HOFFMEYER, J. A., VOGLER, L. E. A new approach to HF channel modeling and simulation. In *Military Communications Conference (MILCOM)*. Monterey (CA, USA), 1990, vol. 3, p. 1199 - 1208.

[8] YANG GUAO, KE WANG A real-time software simulator of wideband HF propagation channel. In *International Conference on Communication Software and Networks*. Macau (China), 2009, p. 304 - 308.

[9] SHEN, Y., MARTINEZ, E. *Channel Estimation in OFDM Systems*, , rev. 1/2006. *Freescale Semiconductor*, 2008.

[10] COLERİ, S., ERGEN, M., PURI, A., BAHAI, A. Channel estimation techniques based on pilot arrangement in OFDM systems, *IEEE Transactions on Broadcasting*, 2002, vol. 48, no. 3.

[11] VAN DE BEEK, J.-J., EDFORS, O., SANDELL, M., WILSON, S. K., BÖRJESSON, P. O. On channel estimation in OFDM systems. In *Proceeding of 45th IEEE Vehicular Technology Conference*. Chicago (IL, USA), 1995, vol. 2, p. 815 - 819.

[12] SANDELL, M., VAN DE BEEK, J.-J., BÖRJESSON, P. O. Timing and frequency synchronization in OFDM systems using the cyclic prefix. In *International Symposium on Synchronization*, 1995, p. 16 - 19.

[13] POLAK, L., KRATOCHVIL, T. Exploring of the DVB-T/T2 performance in advanced mobile TV fading channels. In *36th International Conference on Telecommunications and Signal Processing (TSP2013)*. Rome (Italy), 2013, p. 768 - 772.

[14] MYUNG, H. G., LIM, J., GOODMAN, D. J. Peak-to-average power ratio of single carrier FDMA signals with pulse shaping. In The 17th Annual IEEE International Symposium on Personal, Indoor and Mobile Radio Communications (PIMRC). Helsinki (Finland), 2006, p. 1 - 5.

[15] LIU, Y., TAN, Z. Carrier frequency offset estimation for OFDM systems using repetitive patterns. *Radioengineering*, 2012, vol. 21, no. 3, p. 823 - 830.

[16] TAO, C., QIU, J., LIU, L. A novel OFDM channel estimation algorithm with ICI mitigation over fast fading channels. *Radioengineering*, 2010, vol. 19, no. 2, p. 347 - 355.

About Authors . . .

Fatih GENÇ was born in Ankara, Turkey, in 1984. He received his B.S. degree in July 2007 and M.Sc. in September 2010, in Department of Electronic and Communication Engineering from Çankaya University, Turkey. His research interests include wireless communications, signal processing, HF channels, coding theory, FPGA and DSP. He is currently working for Ph.D. degree at the department of Electronic and Communication Engineering from Çankaya University, Turkey. He is also working at Telecommunications and Signal Processing Laboratory (TESLAB) in Gazi University as a project assistant.

Mustafa Anıl REŞAT was born in Ankara, Turkey, in 1988. He received his B.S. degree in January 2010, in the Department of Electrical and Electronics Engineering, TOBB University of Economics and Technology, Turkey. His research interests include SC-FDMA and OFDMA telecommunication systems, signal processing and high frequency communications. He is currently working for M.Sc. degree at the Department of Electrical and Electronics Engineering, Gazi University, Turkey. He is also working at Telecommunications and Signal Processing Laboratory (TESLAB) in Gazi University as a project assistant.

Asuman YAVANOĞLU has received her B.Sc. and M.Sc. degrees in Electrical Engineering from Erciyes University, Turkey, in 2005 and 2008 respectively. She is currently a Ph.D. student in Electrical and Electronics Engineering specializing in Telecommunications and Signal Processing at Gazi University, Ankara, Turkey, where she is working as a research assistant since 2006. Her research interests include wireless communication systems, MIMO communication and transmit/receive diversity of MIMO-OFDM

Özgür Ertuğ was born in Ankara, Turkey in 1975. He received his B.Sc. degree in 1997 from University of Southern California, USA, M.Sc. degree from Rice University in 1999 and Ph.D. degree from Midddle East Technical University in 2005. He is currently working as assistant professor in Electrical and Electronics Engineering Department of Gazi University. His main research interests lie in algorithm and architecture design as well as theoretical and simulation-based performance analysis of wireless communication systems especially in the physical layer.